DESY-08-152
SFB/CPP-08-72

PROCEEDINGS OF SCIENCE

Hadronic contribution to g-2 from twisted mass fermions

Dru Renner[*†a] **and Xu Feng**[a,b]
[a] *DESY, Platanenallee 6, D-15738 Zeuthen, Germany*
[b] *Universität Münster, Institut für Theoretische Physik, Wilhelm-Klemm-Strasse 9, D-48149 Münster, Germany*
E-mail: dru.renner@desy.de, xu.feng@desy.de

We calculate the vacuum polarization tensor for pion masses from 480 MeV to 270 MeV using dynamical twisted mass fermions at a lattice spacing of 0.086 fm. We analyze the form of the polarization tensor on the lattice using the symmetries of twisted QCD and we study both finite size effects and lattice artifacts at a pion mass of 310 MeV. Results for the lowest order hadronic contribution to g-2 are presented and the impact of systematic errors is discussed.

The XXVI International Symposium on Lattice Field Theory
July 14 - 19, 2008
Williamsburg, Virginia, USA

[*] Speaker.
[†] On behalf of the European Twisted Mass Collaboration.

© Copyright owned by the author(s) under the terms of the Creative Commons Attribution-NonCommercial-ShareAlike Licence.

arXiv:0902.2796v1 [hep-lat] 16 Feb 2009

1. Introduction

The anomalous magnetic moment of the muon, $a_\mu = (g_\mu - 2)/2$, has been both measured and calculated to high precision, possibly revealing a small discrepancy between Nature and the Standard Model. The measurement of the Muon (g-2) Collaboration is $a_\mu^{\rm ex} = 11\,659\,208.0(6.3)10^{-10}$ [1] and has a fractional accuracy of $0.54\cdot 10^{-6}$. The Standard Model value has been estimated by many authors. One recent review [2] quotes a value of $a_\mu^{\rm th} = 11\,659\,179.3(6.8)10^{-10}$, which has just a slightly higher fractional error of $0.58\cdot 10^{-6}$. This results in a discrepancy of $3.1\,\sigma$. Other theoretical estimates produce a range of discrepancies from $0.9\,\sigma$ to $3.4\,\sigma$[1], but in all cases the dominant source of error for the Standard Model calculation is the leading order (in the QED coupling) hadronic contribution, $a_\mu^{\rm had}$. The value quoted in [2], $a_\mu^{\rm had} = 692.1(5.6)10^{-10}$, alone represents 60% of the theoretical error. This quantity is a pure QCD observable and has been shown to be calculable in lattice QCD calculations even in Euclidean space [3].

This hadronic contribution to a_μ is the focus of this work. We present our initial calculation of $a_\mu^{\rm had}$ using two-flavor maximally twisted mass fermions. This is only the second full QCD calculation of this quantity and represents the first such calculation to examine finite size effects and lattice artifacts. As we demonstrate, cleanly controlling all sources of systematic error will be very important to reliably calculate $a_\mu^{\rm had}$.

2. Calculation

The leading order hadronic contribution due to vacuum polarization is

$$a_\mu^{\rm had} = \alpha^2 \int_0^\infty \frac{dq^2}{q^2} w(q^2/m_\mu^2)(\pi(q^2) - \pi(0)) \tag{2.1}$$

where m_μ is the muon mass and $w(q^2/m_\mu^2)$ is given in [3]. The vacuum polarization, $\pi(q^2)$, is determined from the vacuum polarization tensor, $\pi_{\mu\nu}(q)$, by

$$\pi_{\mu\nu}(q) = \int d^4x\, e^{iq\cdot(x-y)} \langle J_\mu(x) J_\nu(y)\rangle = (q_\mu q_\nu - q^2\delta_{\mu\nu})\pi(q^2) \tag{2.2}$$

where $J_\mu(x)$ is the electromagnetic quark current. In particular, we note that the momentum integral in Eq. 2.1 is performed for $q^2 > 0$ [3], thus $\pi(q^2)$ can be calculated directly from lattice QCD. Furthermore, we remark that the momentum integral is peaked at small momentum and the kernel, $w(q^2/m_\mu^2)$, attains a maximal value at $q^2 = (\sqrt{5}-2)m_\mu^2 \approx 0.003$ GeV^2. (The inverse power of q^2 is canceled by the subtraction $\pi(q^2) - \pi(0)$, which is proportional to q^2.) Meanwhile the smallest momentum accessible in our finite volume calculation is $q^2 = (2\pi/L)^2 \approx 0.05$ GeV^2. Therefore a reliable low q^2 extrapolation is essential to calculate $\pi(q^2)$. In particular the ultra-violet subtraction at $q^2 = 0$ required to renormalize $\pi(q^2)$ induces larger uncertainties than naively expected.

[1] The range of values is determined by examining the references given in [2]. The dominant source of this variation is the discrepancy between e^+e^- and τ data used to determine $a_\mu^{\rm had}$.

β	$a\mu$	V/a^4	a	L	m_π	$m_\pi L$	N_{traj}
3.9	0.0100	$24^3 \times 48$	0.086	2.1	480	5.0	120
3.9	0.0085	$24^3 \times 48$	0.086	2.1	450	4.7	207
3.9	0.0064	$24^3 \times 48$	0.086	2.1	390	4.1	139
3.9	0.0040	$24^3 \times 48$	0.086	2.1	310	3.3	178
3.9	0.0030	$32^3 \times 64$	0.086	2.7	270	3.7	101
3.9	0.0040	$32^3 \times 64$	0.086	2.7	310	4.3	124
4.05	0.0030	$32^3 \times 64$	0.067	2.1	310	3.3	104

Table 1: Parameters used in this work. The values of a and L are given in fm and m_π is given in MeV.

3. Lattice Details

We calculate $\pi_{\mu\nu}(q^2)$ using dynamical maximally twisted mass fermions. The twisted quark mass provides an infra-red regulator that bounds the determinant of the fermion action hence eliminating exceptional configurations [4, 5]. Additionally, at maximal twist physical observables are automatically accurate to $\mathcal{O}(a^2)$ in the lattice spacing [6].

The flavor diagonal currents retain their usual form undering twisting.[2] Additionally, in the twisted basis we can use the conserved Noether current instead of the local current. This eliminates the renormalization factor required for the local current and ensures that the Ward identity holds even for non-zero lattice spacing. The conserved current in the twisted basis is given as follows,

$$J^{\text{tw}}_{\mu x} = \frac{1}{2}\left\{\overline{\chi}^{\text{tw}}_{x+\hat{\mu}}(r+\gamma_\mu)U^\dagger_{\mu,x}\chi^{\text{tw}}_x - \overline{\chi}^{\text{tw}}_x(r-\gamma_\mu)U_{\mu,x}\chi^{\text{tw}}_{x+\hat{\mu}}\right\}$$

and has the same point-split form as the standard Wilson current. This can be understood easily once one realizes that both the Wilson mass term and the twisted mass term are invariant under local QED gauge transformations and hence do not contribute to the Noether construction of the conserved current.

The calculation of $\pi_{\mu\nu}(q^2)$ proceeds as for Wilson and domain wall fermions. Propagators from point sources at a single site and the four forward neighbors are calculated and used to construct the current-current correlator in Eq. 2.2. The one exception is that separate u and d quark inversions must be performed due to the modified γ_5-hermiticity: $\gamma_5 D_u^\dagger \gamma_5 = D_d$.[3]

Twisted fermions break flavor symmetry. However, the γ_5-hermiticity relates u and d quark loops and results in $\pi^d_{\mu\nu}(x,y) = \pi^{u*}_{\mu\nu}(x,y)$. This expression is true for each gauge field configuration. The consequence is that $\text{re}(\pi^d(q^2)) = \text{re}(\pi^u(q^2))$. Hence by simply taking the real part of $\pi(q^2)$, which is real in the continuum limit, we eliminate any explicit flavor breaking in the valence sector. Additionally, we expect the real part of π to be accurate to $\mathcal{O}(a^2)$, even if the imaginary part has $\mathcal{O}(a)$ corrections.

In this work we use the two-flavor dynamical gauge field configurations from the European Twisted Mass Collaboration [7–9]. The details of the ensembles used are given in Tab. 1. Additionally, the hadronic contribution to a_μ has previously been calculated using quenched domain

[2] This follows simply from $Q\gamma_\mu = \exp(-i\gamma_5\tau_3\theta)Q\gamma_\mu\exp(-i\gamma_5\tau_3\theta)$ for $Q = 1$ and τ_3.

[3] This can be seen from the basic loop expression $\gamma_\mu D_u^{-1}(x,y)\gamma_\nu D_u^{-1\dagger}(y,x) = \gamma_\mu D_u^{-1}(x,y)\gamma_\nu\gamma_5 D_d^{-1}(x,y)\gamma_5$.

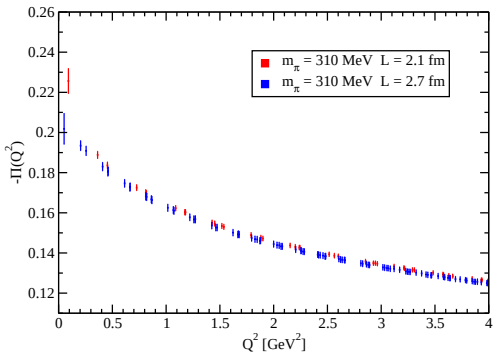

Figure 1: Volume dependence of $-\pi(q^2)$. This quantity requires an ultra-violet subtraction but is infra-red finite. With the exception of the lowest q^2 point, there is no noticeable finite size effect.

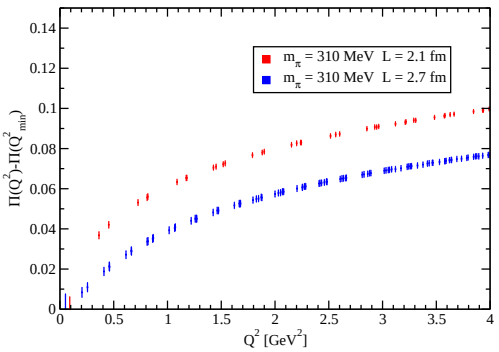

Figure 2: Volume dependence of $\pi(q^2) - \pi(0)$. As an illustration, this quantity is renormalized at the lowest momentum accessible in each volume, demonstrating the sensitive nature of the subtraction.

wall fermions [3], quenched improved Wilson fermions [10] and dynamical rooted asqtad improved staggered fermions [11].

4. Results

First we examine the finite size effects in $\pi(q^2)$. We have calculated it at two volumes, $L =$ 2.1 fm and $L = 2.7$ fm, both with $m_\pi = 310$ MeV and $a = 0.086$ fm. In Fig. 1 we show the results for $\pi(q^2)$ for these two volumes. Although $\pi(q^2)$ is an ultra-violet divergent quantity, for a fixed a we expect a finite large volume limit. Fig. 1 demonstrates this rather clearly for all but the lowest q^2 point. However, the ultra-violet subtraction required to form a_μ exaggerates any differences at low q^2. Fig. 2 illustrates this point. Determining $\pi(0)$ requires a fit, so for the purposes of illustration we perform the subtraction at the lowest q^2 value available for each of the two volumes. Fig. 2 demonstrates that this subtraction can have a large effect on the resulting renormalized quantity. However, the integral in Eq. 2.1 is dominated by the region near $q^2 \approx 0.003$ GeV^2 and hence is not fully sensitive to the overall shift in Fig. 2.

Next we study the m_π dependence. Figs. 3 and 4 show all five values of m_π for $a = 0.086$ fm. In the case of $m_\pi = 310$ MeV, only the larger $L = 2.7$ fm results are shown. Fig. 3 demonstrates that there is no visible quark mass dependence for large q^2, as expected from perturbation theory. Any quark mass dependence should be more visible for the low q^2 region shown in Fig. 4. The error bars are too large to identity any quark mass dependence, however, the results do appear to systematically increase when proceeding from the $m_\pi = 450$ MeV calculation down to the 270 MeV result.

Now we examine the lattice artifacts in $\pi(q^2)$. We have calculated at two lattice spacings, $a = 0.086$ fm and $a = 0.067$ fm. In both cases we have taken $m_\pi = 310$ MeV and $L = 2.1$ fm. Fig. 5 shows the unrenormalized results for $\pi(q^2)$ demonstrating the ultra-violet divergence present without the subtraction. In Fig. 6 we perform the subtraction, but at $q^2 = 0.3$ GeV^2 rather than at $q^2 = 0$. We see no noticeable lattice artifacts with the exception of the lowest q^2 point. Unfortunately the

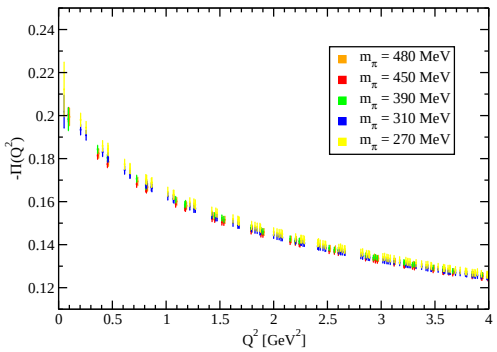

Figure 3: Quark mass dependence at large q^2. There is no noticeable quark mass dependence at large q^2, consistent with perturbative QCD expectations.

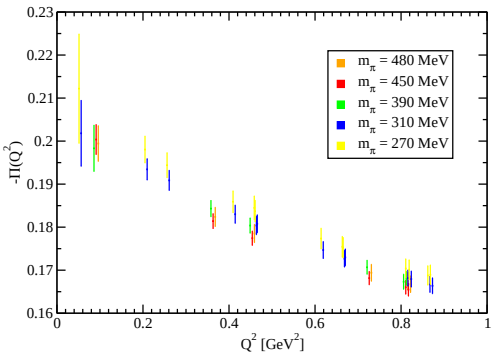

Figure 4: Quark mass dependence at low q^2. There is a systematic, but not statistically significant, shift with quark mass from $m_\pi = 450$ MeV to 270 MeV.

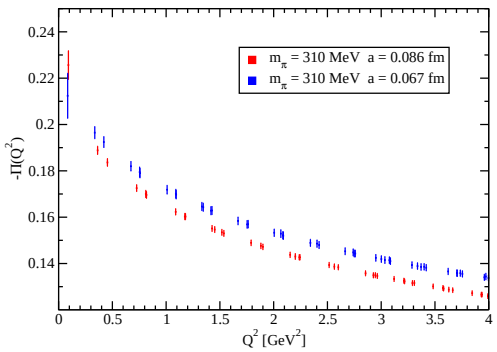

Figure 5: Lattice spacing dependence of $-\pi(q^2)$. The unrenormalized $-\pi(q^2)$ is shown. The discrepancy illustrates the ultra-violet subtraction required to renormalize π.

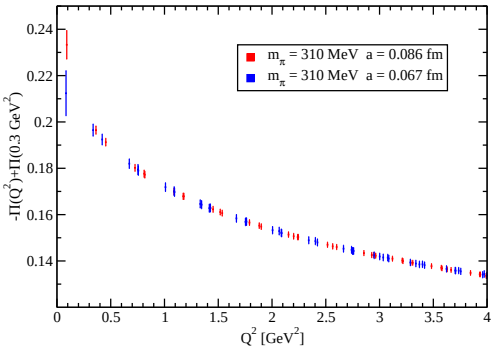

Figure 6: Lattice spacing dependence of $-\pi(q^2)$ matched at $q^2 = 0.3$ GeV^2. With the exception of the lowest q^2 point, there is no noticeable lattice spacing dependence.

expression for a_μ in Eq. 2.1 requires the subtraction at $q^2 = 0$. This is shown in Fig. 7 where, as earlier, we subtract at the lowest q^2 point available in each calculation. Again, the subtraction induces a large difference between the results from the two lattice spacings, but we must remember that a_μ is dominated by values of q^2 around 0.003 GeV^2.

To determine the extent to which the effects shown in Figs. 2 and 7 contribute to $a_\mu^{\rm had}$, we must parametrize and fit $\pi(q^2)$ and extrapolate to $q^2 = 0$ in order to perform the integral in Eq. 2.1. In Fig. 8 we show fits to polynomials in q^2 with 4 terms (cubic) and 5 terms (quartic). The lattice results and corresponding curves are shifted vertically to illustrate the quality of the fits and the nature of the extrapolation to $q^2 = 0$. Additionally, the calculation labeled $m_\pi = 310$ MeV refers to the larger $L = 2.7$ fm calculation. For all but one ensemble the cubic fit seems sufficient to describe the lattice results. The one exception is the $m_\pi = 310$ MeV, smaller volume $L = 2.1$ fm calculation (not shown), which requires the quartic term to accommodate the observed low q^2 behavior.

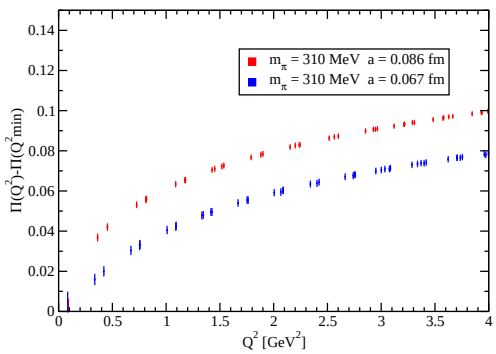

Figure 7: Lattice spacing dependence of $\pi(q^2) - \pi(0)$. The results have been renormalized at the lowest value of q^2 at each lattice spacing to illustrate the effect of the subtraction.

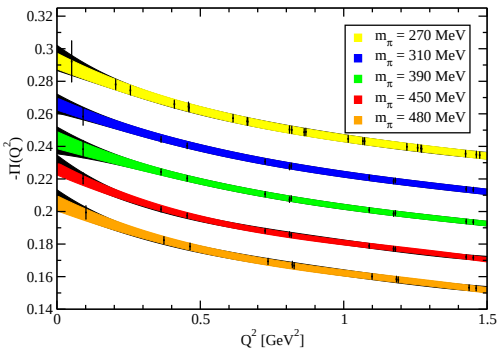

Figure 8: Low q^2 extrapolation. Each $\pi(q^2)$ has been fit to cubic (foreground) and quartic (background) functions of q^2, showing agreement for all but the smaller volume at 310 MeV (not shown).

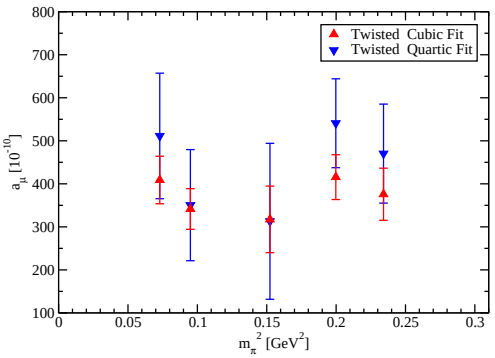

Figure 9: Comparison of cubic and quartic fit results for $a_\mu^{\rm had}$. There is general agreement between the cubic and quartic fits for all calculations excluding the smaller volume at $m_\pi = 310$ MeV (not shown).

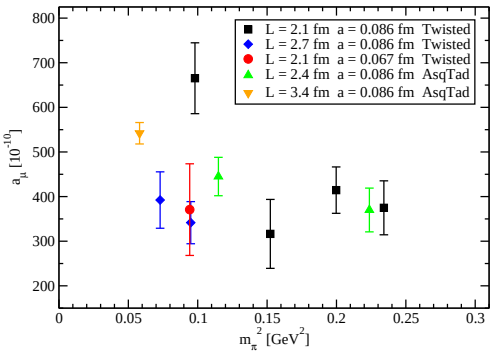

Figure 10: Comparison of all full QCD calculations of $a_\mu^{\rm had}$. The results of this work are shown along with the staggered results of [11]. Finite size effects and lattice artifacts are visible.

Using the fits described above, we calculate $a_\mu^{\rm had}$ using Eq. 2.1. Fig. 9 shows the resulting values for the five masses at $a = 0.086$ fm. (Again the larger value of $L = 2.7$ fm is used for $m_\pi = 310$ MeV.) We note a clear consistency between the cubic and quartic fits as already indicated in Fig. 8. Additionally, there is no discernible quark mass dependence as implied by Figs. 3 and 4. In Fig. 10, we focus specifically on the cubic fits and examine the L and a dependence of our results and we compare to the only other full QCD calculation [11][4]. First we notice the quite large finite size effects and lattice artifacts as anticipated in Figs. 2 and 7. However, in general we find consistency with the staggered results. The agreement for the largest staggered value of m_π is quite clear. The intermediate staggered value is at a volume that is between our larger and smaller volumes, and the result also lies between our two results. This seems quite consistent to within the

[4] We will refer to the results in [11] as staggered and have taken the results corresponding to the cubic fits in [11].

systematic errors that we observe near this value of m_π. Finally $a_\mu^{\rm had}$ at the lightest staggered value of m_π appears to be a bit too high compared to our lightest value. This might be genuine quark mass dependence, but given the strength of finite size effects and lattice artifacts that we observe, we find it difficult to claim a strong quark mass dependence. In fact the sign of the discrepancy is consistent with both a finite size effect, which should be universal, and also with our lattice artifacts, which, though not universal, might still be indicative.

5. Conclusions

The current high precision determinations of the anomalous magnetic moment, a_μ, both from experiment and theory, indicate a small discrepancy between Nature and the Standard Model. The largest source of error in the theory calculation of a_μ is the leading order hadronic contribution. We present a full QCD calculation of the vacuum polarization and, in particular, of precisely this hadronic contribution. We perform calculations with dynamical maximally twisted mass fermions with pion masses ranging from 480 MeV to 270 MeV. We observe both large finite size effects and lattice artifacts but find general agreement with the only other full QCD calculation. This work presents the first full QCD calculation of these effects and represents a first effort to begin to calculate a_μ controlling for all sources of error.

6. Acknowledgments

We thank Karl Jansen and Carsten Urbach for their valuable suggestions and assistance and Giancarlo Rossi and Gregorio Herdoiza for their comments on the proceedings. We thank the John von Neumann Institute for Computing (NIC) for computing resources and the staff at the Jülich Supercomputing Center and DESY Zeuthen Computing Center for their support. This work has been supported in part by the DFG Sonderforschungsbereich/Transregio SFB/TR9-03 and the DFG project Mu 757/13.

References

[1] G. W. Bennett et al. *Phys. Rev.*, D73:072003, 2006.

[2] F. Jegerlehner. *Acta Phys. Polon.*, B38:3021, 2007.

[3] T. Blum. *Phys. Rev. Lett.*, 91:052001, 2003.

[4] R. Frezzotti, P. A. Grassi, S. Sint, and P. Weisz. *Nucl. Phys. Proc. Suppl.*, 83:941–946, 2000.

[5] R. Frezzotti, P. A. Grassi, S. Sint, and P. Weisz. *JHEP*, 08:058, 2001.

[6] R. Frezzotti and G. C. Rossi. *JHEP*, 08:007, 2004.

[7] Ph. Boucaud et al. *Phys. Lett.*, B650:304–311, 2007.

[8] Ph. Boucaud et al. arXiv:0803.0224, 2008.

[9] Carsten Urbach. *PoS*, LAT2007:022, 2007.

[10] M. Gockeler et al. *Nucl. Phys.*, B688:135–164, 2004.

[11] C. Aubin and T. Blum. *Phys. Rev.*, D75:114502, 2007.